Mathematical Modeling: Magnetic Field Effect on Oscillatory MHD Couette Two Dimensional Flow Regime

Alok Singh, Savita Singh and Sudhir Kumar Sharma

June 22, 2022

Mathematical Modeling: Magnetic Field Effect on Oscillatory MHD Couette Two Dimensional Flow Regime

Alok Singh[a] , Savita Singh[b] , Sudhir Kumar Sharma[c]

[a,b,c]*Department of Physics, Harcourt Butler Technical University, Kanpur-208002, India.*

Abstract

In this paper, a mathematical modeling with quantitative analysis of oscillatory MHD Couette flow between two parallel plates (upper plate is moving relative to fixed lower plate) has been performed by using perturbation technique. The key parameters of this quantitative analysis are velocity gradient, viscosity, magnetic field, amplitude of shear stress, phase lag of shear stress, and frequency of pulsating flow. The mathematical modeling analysis revealed that the amplitude of velocity gradient increases at lower plate comparative to upper plate with increasing magnetic field while the amplitude of shear stress decreases rapidly with increasing magnetic field and becomes constant beyond higher values. This mathematical modeling with quantitative analysis can be utilised in various engineering fields for instance magnetorheological dampers, magnetorheological finishing in optics, enhanced body armor in military and defense, automotive, aerospace, human prosthesis, magneto-hydrodynamics power generators and pumps, polymer technology, petroleum industry.

Keywords: MHD; Harmonic oscillation; Rate of heat transfer; Magnetic field oscillatory flow.

1. Introduction

Over the past decade or so, the problem of time-dependent oscillatory flow in which fluctuating part of the motion is superimposed on mean steady parts was studied by several research group [1-4]. The magnetic analogue of Light hill's investigation led to an increase of the oscillatory flow based research on small harmonic oscillation in a channel of gap 'h'. The analysis of unsteady flow of the stream with its conjugate complex part concluded that the amplitude of the fluctuating velocity gradient varies with respect to transverse magnetic field [5-6].

In recent years, oscillatory free convective flow and heat transfer problem in the presence of a magnetic field through a porous composite or medium have attracted the attention of many researchers due to their possible engineering application [7-9]. In practice, cooling of porous structure is achieved by forcing the liquid or gas through capillaries of solid. Actually, they were used to insulate a heated body to maintain its temperature. Study of origin of flow through a porous medium is heavily based on Darcy’s experimental law. In view of Darcy’s law, Yamamoto and Yoshida, Hooper et al considered suction and injection flow with convective acceleration through a plane porous wall especially for the flow outside a vertex layer [10-12]. The oscillatory flow past a porous bed have presented the study of two-dimensional flow of viscous fluid through a porous medium bounded by a porous surface subject to a constant suction velocity by taking account of free convection currents [13-15].

A magnetorheological fluid is a smart fluid usually a type of oil. The magnetic field of electromagnets can control magnetorheological fluids filled in dampers for shock observer. A magnetorheological fluid has three main modes of operation: flow mode, shear mode and squeeze flow mode. This fluid between two parallel plates moving relative to one another and fluid between two plates moving in the direction perpendicular direction to their planes with perpendicular magnetic fields to their planes [16].

The objective of this presented research work is to develop mathematical model for fluid flow in order to understand and predict the behavior of magnetorheological fluid. In this presented research work, a mathematical modeling with quantitative analysis of oscillatory MHD Couette flow between two parallel plates (upper plate is moving relative to fixed lower plate) has been performed in terms of constitutive parameters using perturbation theory. The dependency of constitutive parameters and its variations are mathematical calculated and analysed.

2. Mathematical Analysis

Consider a two – dimensional oscillating flow of an incompressible fluid with constant properties and magnetic field is applied between two parallel flat walls, one of which is at rest and other moving in its own plane with an unsteady low velocity as shown in Fig. 1. The restriction of this case is that the flow is independent of the distance along the wall and the velocity component normal to the wall is zero.

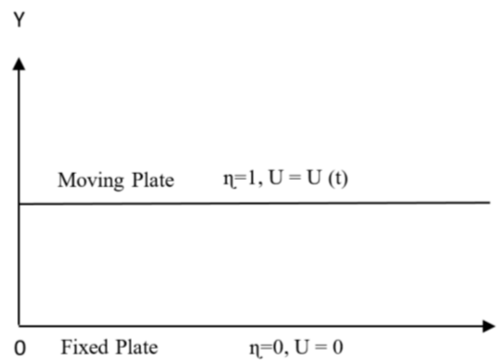

Fig. 1. Systematic of two dimensional flow of an incompressible fluid.

The momentum of fluid flow or inertial force of fluid can be neglected in comparison to the viscous force at low fluid velocity in the Navier-Stokes equation of motion. The Couette flow motion is introduced here due to the movement of the upper plate which can be represented as [17],

$$\frac{\partial u}{\partial t} = -\frac{1}{\rho}\frac{\partial p}{\partial x} + \vartheta\frac{\partial^2 u}{\partial y^2} - \frac{\sigma B_0^2}{\rho}u \quad (1)$$

$$0 = -\frac{1}{\rho}\frac{\partial p}{\partial y} \quad (2)$$

The fixed plate is along x-axis and y-axis is normal to it. Plates are at distance 'h' apart. The expression of unsteady velocity between the plates is given by [17],

$$U(t) = U_h[1 + \frac{t}{2}(e^{iwt} + e^{-iwt})] \quad (3)$$

Where ω is the frequency and U_h and t are constants.

We considered the solution of equation (1) as [17],

$$u = U_h[u_0(\eta) + \frac{t}{2}\{u_1(\eta)e^{i\omega t} + \overline{u_1}(\eta)e^{-i\omega t}\}] \quad (4)$$

Where $\eta = \frac{y}{h}$. On substituting equation (3) and (4) in equation (1) and equating steady and unsteady parts, we have [17],

$$u_0^{"} = 0 \quad (5)$$

$$u_1^{"} - (m + ik)u_1 = -(m + ik) \quad (6)$$

The boundary conditions are [17],

$$\eta = 0, u_0 = u_1 = 0; \eta = 1, u_0 = u_1 = 1 \tag{7}$$

where, $m = \frac{\sigma B_0^2}{\rho}\frac{h^2}{\nu}$ and $k = \frac{\omega h^2}{\upsilon}$ are magnetic and frequency parameters respectively.

Equations (5) and (6) are simple linear differential equations, whose complementary and particular solutions are constituted as:

The solution of equation (5) is,

$$u_0 = \eta \tag{8}$$

The solution of equation (6) is [17],

$$u_1 = 1 - \cosh(m+ik)^{\frac{1}{2}}\eta + \coth(m+ik)^{\frac{1}{2}}\sinh(m+ik)^{\frac{1}{2}}\eta \tag{9}$$

The magnitude of the fluctuating velocity gradient at lower wall is [17],

$$|u_1'| = \frac{2}{(\cosh 2\theta_1 - \cosh 2\theta_2)}(\theta_1^2 + \theta_2^2)^{\frac{1}{2}}(\sinh^2 2\theta_1 + \sinh^2 2\theta_2)^{\frac{1}{2}} \tag{10}$$

The magnitude of the fluctuating velocity gradient at mid plane is [17],

$$|u_1'| = \frac{2}{(\cosh 2\theta_1 - \cosh 2\theta_2)}(\theta_1^2 + \theta_2^2)^{\frac{1}{2}}(\sinh^2 2\theta_1 + \sinh^2 2\theta_2)^{\frac{1}{2}} \times (\cosh^2\frac{\theta_1}{2}\cos^2\frac{\theta_2}{2} + \sinh^2\frac{\theta_1}{2}\sin^2\frac{\theta_2}{2})^{\frac{1}{2}} \tag{11}$$

The magnitude of the fluctuating velocity gradient at upper wall is [17],

$$|u_1'| = \frac{2}{(\cosh 2\theta_1 - \cosh 2\theta_2)}(\theta_1^2 + \theta_2^2)^{\frac{1}{2}}(\sinh^2\theta_1\cos^2\theta_2 + \cosh^2\theta_1\sin^2\theta_2)^{\frac{1}{2}} \tag{12}$$

Where $\theta_1 = (m^2 + k^2)^{\frac{1}{4}}\cos\alpha$, $\theta_2 = (m^2 + k^2)^{\frac{1}{4}}\sin\alpha$ and $\alpha = \frac{1}{2}\tan^{-1}\frac{k}{m}$.

The shear stress at $y = 0$ is given by,

$$T_w = \mu\left(\frac{\partial u}{\partial y}\right)_{y=0}$$

$$T_w = \frac{\mu U_h}{h}\{1 + \frac{t}{2}(Ae^{i\omega t} + \bar{A}e^{-i\omega t})\} \tag{13}$$

Where, $A = (m+ik)^{\frac{1}{2}}\coth(m+ik)^{\frac{1}{2}}$ (14)

An expression of the amplitude of shear stress of lower wall is given by,

$$|A| = \frac{2}{(\cosh 2\theta_1 - \cosh 2\theta_2)^{\frac{1}{2}}}(\theta_1^2 + \theta_2^2)^{\frac{1}{2}}(\sinh^2 2\theta_1 + \sinh^2 2\theta_2)^{\frac{1}{2}} \tag{15}$$

An expression of the phase angle of shear stress of lower wall is given by,

$$\psi = \tan^{-1}\left[\frac{\theta_2\sin 2\theta_1 - \theta_1\sinh 2\theta_2}{\theta_1\sin 2\theta_1 - \theta_2\sinh 2\theta_2}\right] \tag{16}$$

2.1. Temperature Field

Under the flow conditions, the equations for the temperature distribution with negligible heat generation due to Joule's effect is [17],

$$\frac{\partial T}{\partial t}+u\frac{\partial T}{\partial x}=K\left(\frac{\partial^2 T}{\partial x^2}+\frac{\partial^2 T}{\partial y^2}\right)+\frac{\upsilon}{c}\left(\frac{\partial u}{\partial y}\right)^2 \tag{17}$$

In this case, x-denotes the distance along the wall, T is the temperature, K is the thermal diffusivity and C is the specific heat.

The following boundary condition were used to solve equation,

$$\mathrm{T}=\mathrm{T_w} \text{ or } \frac{\partial T}{\partial y}=0 \text{ at } y=0$$

$$T=T_h \text{ at } y=h \tag{18}$$

With these boundary conditions the solution obtained is independent of x. In the present case, the heat transferred due to convection is negligible. Temperature distribution is caused only due to conduction and viscous dissipation.

Thus, we have,

$$\frac{\partial T}{\partial t}=K\frac{\partial^2 T}{\partial y^2}+\frac{\nu}{c}\left(\frac{\partial u}{\partial y}\right)^2 \tag{19}$$

Looking for the solution of equation (19) in the form as,

$$T(\eta)=T_0(\eta)+\frac{1}{2}\varepsilon\left[T_1(\eta)e^{i\omega t}+\overline{T_1}(\eta)e^{-i\omega t}\right]+\frac{1}{2}\varepsilon^2\left[T_2(\eta)e^{2i\omega t}+\overline{T_2}(\eta)e^{-2i\omega t}\right] \tag{20}$$

Equating the harmonic coefficients to zero, we have

$$T_0^{''}=-\frac{P_r U_h^2}{c} \tag{21}$$

$$T_1^{''}-iP_r kT_1=-\left(\frac{P_r U_h^2}{c}\right)u_0^{'}u_1^{'} \tag{22}$$

where $P_r=\frac{\mu c}{k}$ is the Prandtle number, $k=\frac{\omega h^2}{\nu}$ is frequency parameter.

The boundary conditions reduce to as,

$$T_0=T_\omega\ , T_1=T_2=0 \text{ at } \eta=0$$

$$T_0=T_h\ , T_1=T_2=0 \text{ at } \eta=1 \tag{23}$$

The solution of equation (22) and (23) are

$$\frac{T_0-T_h}{T_\omega-T_h}=-P_r E\frac{\eta}{2}(\eta-1)+\eta+1 \tag{24}$$

$$\frac{T_1}{T_\omega-T_h}=P_r E\frac{l}{(l^2-I^2)}\left[\sinh l\eta(\mathrm{cosechIcoshl}+1)+\coth l(\mathrm{cosechIcoshI}(1-\eta)+\cosh l\eta)\right] \tag{25}$$

where, $l^2=m+ik$, $I^2=iP_r k$ and $E=\frac{U_h^2}{c(T_\omega-T_h)}$ is Eckert number.

The rate of heat transfer is given as,

$$\frac{T_1^{'}(\eta)}{T_\omega - T_h} = P_r E \frac{l}{I(l^2 - I^2)}\left[\frac{\cosh l\eta}{l}(\text{cosechIcoshl}+1) - \coth l(\text{cosechIcoshI}\,\frac{(1-\eta)}{\text{I}} + \frac{\sinh l\eta}{l})\right] \quad (26)$$

The rate of heat transfer at lower plate is given by,

$$\frac{T_1^{'}(0)}{T_\omega - T_h} = \frac{P_r E}{I(l^2 - I^2)}[I + \text{cosechIcoshl}(I - l\text{cosechloshI})] \quad (27)$$

The rate of heat transfer at upper plate is given by,

$$\frac{T_1^{'}(1)}{T_\omega - T_h} = \frac{P_r E}{I(l^2 - I^2)}\frac{\coth l}{2\sinh l}[I\sinh 2l - 2l] \quad (28)$$

3. Results and Discussion

The significance of magnetic field is that it controls the flow of fluid between two parallel plates while frequency parameter of pulsating flow perturb the other constitutive parameters. The distribution of the magnitude of fluctuating velocity gradient $|u_1{}'|$ are shown in Table 1 and figure 2 for several values of m and at fixed value of frequency parameter. Variation of the amplitude and phase lag of the shear stress at lower wall with respect to magnetic field parameter for fixed value of frequency parameter has been shown in Table 2 and variation of the amplitude and phase lag of the shear stress shown in figure 3. The amplitude of shear stress decreases rapidly between m=1 and m=2, then after it becomes constant with magnetic field parameter.

Several values of frequency parameter for lower wall with fixed value of magnetic field parameter has been shown in Table 3. We observe that amplitude of the shear stress at lower plate increases with increasing frequency parameter for fixed magnetic field parameter while, phase lag increases with magnetic field parameter increases as shown in Figure 5 and Figure 4 respectively. Moreover, we observe that the phase lag decreases with increasing frequency parameter as shown in Figure 6.

The amplitude and phase lag of rate of heat transfer at lower plate increases with increasing magnetic field parameter. However, the amplitude and phase lag of rate of heat transfer at upper plate is same at lower plate. These variations are shown in Table 4 and Table 5.

Table 1. Variation of fluctuating velocity gradient with η. For fixed value K = 1.

m \ η	$\lvert u_1' \rvert$		
	0.0	**0.5**	**1.0**
0	0.09	0.25	0.20
1	2.70	0.61	0.52
2	3.33	0.94	0.73
3	3.79	1.15	0.83
4	4.20	1.98	0.95
5	5.01	2.32	1.02
6	5.98	3.01	2.31
7	6.02	3.99	3.12
8	6.99	4.20	4.05
9	7.73	5.39	5.13
10	8.08	6.17	6.09

Table 2. Variation of amplitude and phase lag of the shear stress at lower wall. For fixed value m = 2.

S.No.	**K**	$\|A\|$	Ψ
1.	1	0.3880	72.8051
2.	2	1.5694	60.6989
3.	3	2.3435	52.8321
4.	4	4.3413	49.3235
5.	5	5.8898	40.3135

Table 3. Variation of amplitude and phase lag of the shear stress at lower wall. For fixed value K = 2.

S.No.	**m**	$\|A\|$	Ψ
1.	1	43.2995	31.9641
2.	2	4.8000	49.2559
3.	3	1.8000	53.9830
4.	4	1.6000	61.3257
5.	5	1.6000	74.5323

Table 4. Heat transfer variation at lower wall with respect to magnetic field parameter m. Pr =2, E = 10, K = 5.

S.No.	**m**	$\frac{T_1'(0)}{T_w - T_h}$	$\|\beta_1\|$	$\emptyset_1$
1.	1	9.2631- i1.5032	9.3842	10.2416
2.	5	5.2140+ i 10.5660	11.7824	70.8167
3.	10	1.2315+ i 15.3216	15.3710	94.8940

Table 5. Heat transfer variation at upper wall with respect to magnetic field parameter m. Pr =2, E = 10, K = 5.

S.No.	**m**	$\frac{T_1'(1)}{T_w - T_h}$	$\|\beta_2\|$	$\emptyset_2$
1.	1	7.6567- i0.3548	7.6649	2.9478
2.	5	10.5204+ i 8.6241	13.6034	43.7146
3.	10	14.5109+ i 13.0990	19.5486	46.7473

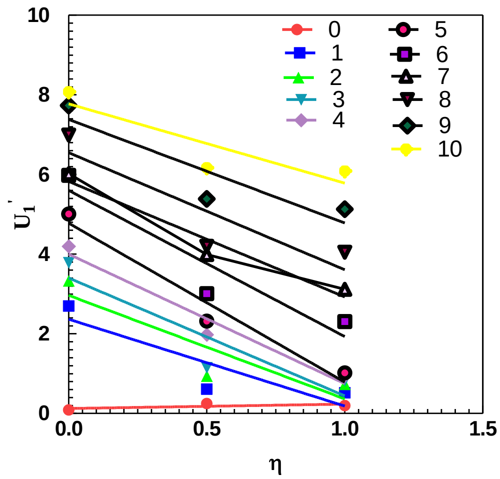

Fig. 2. The distribution of fluctuating velocity gradient verses η.

The Fig. 2. illustrates that the higher rate of increase in amplitude of fluctuating velocity gradient with increasing magnetic field parameter at lower plate than upper plate at fixed frequency parameter. A significant increase in velocity gradient occurs above magnetic field parameter m=4.

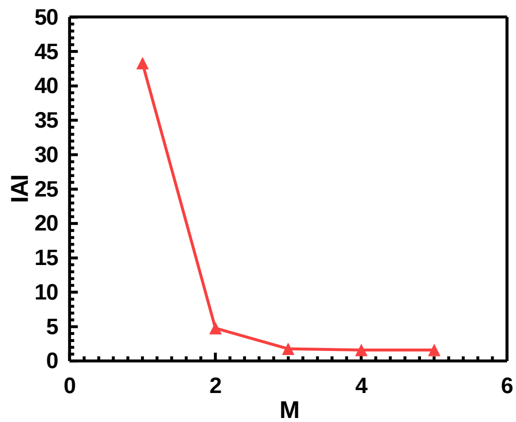

Fig. 3. The distribution of amplitude of shear stress with magnetic field parameter.

The Fig. 3. shows that the amplitude of shear stress decrease rapidly with increasing magnetic field parameter between 0 to 2 value but, beyond the value m=3 becomes constant.

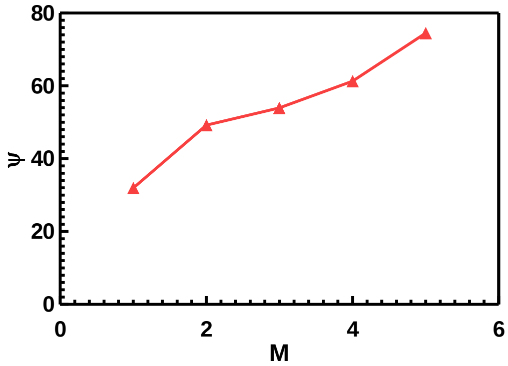

Fig. 4. Variation of phase lag of shear stress with magnetic field parameter.

The Fig. 4. indicates almost linear increment with increasing magnetic field parameter.

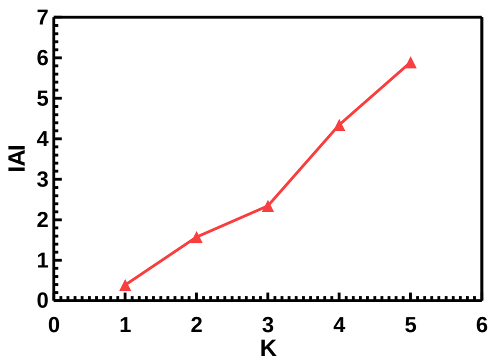

Fig. 5. Variation of amplitude of shear stress with frequency parameter.

The Fig. 5. illustrates that amplitude of shear stress with increasing frequency parameter beyond the value of unity.

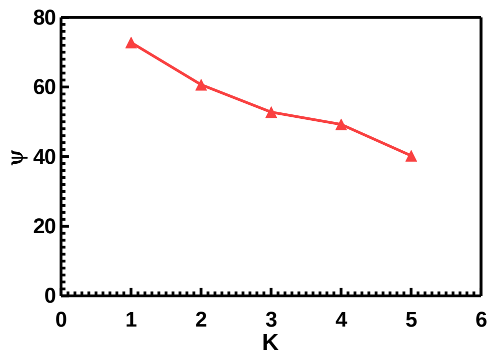

Fig. 6. Variation of phase lag of shear stress with frequency parameter.

Fig. 6. illustrates a linear decrement of the phase lag with increasing frequency parameter.

4. Conclusions

This paper presents a mathematical modeling with quantitative analysis of oscillatory MHD Couette flow using perturbation theory. A set of modeled expression of the amplitude and phase angle of shear stress of lower wall have been developed mathematically [Eq. (15) and Eq. (16)]. Moreover, mathematical modeled expression for the rate of heat transfer at lower plate and upper plate have been also developed [Eq. (27) and Eq. (28)]. It has been concluded that the amplitude of shear stress decreases rapidly between m=1 and m=2, then after it becomes constant with magnetic field parameter while, the amplitude of the shear stress at lower plate increases with increasing frequency magnetic field. However, phase lag increases with increasing magnetic field but, it decreases with increasing frequency parameter. The amplitude and phase lag of rate of heat transfer at lower plate increases with increasing magnetic field which is equal at upper and lower plate. This mathematical modeling with quantitative analysis can be utilised in various engineering fields for instance magnetorheological dampers, magnetorheological finishing in optics, enhanced body armor in military and defense, automotive, aerospace, human prosthesis, magneto-hydrodynamics power generators and pumps, polymer technology, petroleum industry.

In future, these developed mathematical models can be analysed for validation in Nano-fluid dynamics, Polymer fluid dynamics, paraffin oil fluid dynamics, oil and paint technology, etc.

References:

[1] Lighthill MJ. The response of laminar skin friction and heat transfer to fluctuations in the stream velocity. Proceedings of the Royal Society of London. Series A. Mathematical and Physical Sciences. 1954;224(1156):p.1-23.

[2] Scotti A, Piomelli U. Numerical simulation of pulsating turbulent channel flow. Physics of Fluids. 2001;13(5):p.1367-84.

[3] Soundalgekar VM, Wavre PD, Takhar HS. Effects of free convection currents on the oscillatory flow of an electrically conducting fluid past a stationary or steadily moving vertical plate with variable suction and constant heat flux. International journal of applied mechanics and engineering. 2001;6(3):p.639-58.

[4] Riley N. Steady streaming. Annual review of fluid mechanics. 2001;p.33:43.

[5] Šidlof P, Zörner S, Hüppe A. A hybrid approach to the computational aeroacoustics of human voice production. Biomechanics and modeling in mechanobiology. 2015;14 (3):p.473-88.

[6] Hanratty TJ, Campbell JA. Measurement of wall shear stress. In Fluid mechanics measurements 2017; 13: p. 575-648.

[7] Varsakelis C, Papalexandris MV. Numerical study of unsteady shear, and gravity-driven granular flows. Bulletin of the American Physical Society. 2011 22;p.56.

[8] Noranuar WN, Mohamad AQ, Shafie S, Khan I, Jiann LY, Ilias MR. Non-coaxial rotation flow of MHD Casson nanofluid carbon nanotubes past a moving disk with porosity effect. Ain Shams Engineering Journal. 2021 ;12(4):p.4099-110.

[9] M'hamed B, Sidik NA, Yazid MN, Mamat R, Najafi G, Kefayati GH. A review on why researchers apply external magnetic field on nanofluids. International Communications in Heat and Mass Transfer. 2016 ;78:p.60-7.

[10Yamamoto K, Yoshida ZI. Flow through a porous wall with convective acceleration. Journal of the Physical Society of Japan. 1974 Mar;37(3):774-9.

[11] Yamamoto K, Iwamura N. Flow with convective acceleration through a porous medium. Journal of Engineering Mathematics. 1976 ;10(1):p.41-54.

[12] Zeghari K, Louahlia H, Le Masson S. Experimental investigation of flat porous heat pipe for cooling TV box electronic chips. Applied Thermal Engineering. 2019; 25;163: p.114267.

[13] Ahmed S, Kalita K. Analytical and numerical study for MHD radiating flow over an infinite vertical surface bounded by a porous medium in presence of chemical reaction. Journal of Applied Fluid Mechanics. 2013;6 (4):p.597-607.

[14] Sharma BK, Yadav K, Mishra NK, Chaudhary RC. Soret and Dufour effects on unsteady MHD mixed convection flow past a radiative vertical porous plate embedded in a porous medium with chemical reaction. Applied Mathematics .2012;3(7):p.717-723.

[15] Sharma PK. Simultaneous thermal and mass diffusion on three-dimensional mixed convection flow through a porous medium. Journal of Porous Media. 2005;8(4).

[16] Hua D, Liu X, Li Z, Fracz P, Hnydiuk-Stefan A, Li Z. A review on structural configurations of magnetorheological fluid based devices reported in 2018–2020. Frontiers in Materials. 2021;8: p.640102.

[17] Batchelor CK, Batchelor GK. An introduction to fluid dynamics. Cambridge university press; 2000 Feb 28.